IEEE Access
Multidisciplinary | Rapid Review | Open Access Journal

Received November 26, 2020, accepted January 7, 2021, date of publication January 14, 2021, date of current version January 22, 2021.

Digital Object Identifier 10.1109/ACCESS.2021.3051642

Evaluation of the ERA5 Sea Surface Temperature Around the Pacific and the Atlantic

LING YAO[1,2,4], JIAYING LU[1,2,3], XIAOLIN XIA[2,5], WENLONG JING[2,5], AND YANGXIAOYUE LIU[2,5]

[1]State Key Laboratory of Resources and Environmental Information System, Institute of Geographic Sciences and Natural Resources Research, Chinese Academy of Sciences, Beijing 100101, China
[2]Southern Marine Science and Engineering Guangdong Laboratory, Guangzhou 511458, China
[3]College of Resources and Environment, University of Chinese Academy of Sciences, Beijing 100101, China
[4]Jiangsu Center for Collaborative Innovation in Geographical Information Resource Development and Application, Nanjing Normal University, Nanjing 210023, China
[5]Guangdong Open Laboratory of Geospatial Information Technology and Application, Key Laboratory of Guangdong for Utilization of Remote Sensing and Geographical Information System, Engineering Technology Center of Remote Sensing Big Data Application of Guangdong Province, Guangzhou Institute of Geography, Guangzhou 510070, China

Corresponding author: Wenlong Jing (jingwl@lreis.ac.cn)

This work was supported in part by the National Natural Science Foundation of China under Grant 41771380, in part by the Key Special Project for Introduced Talents Team of Southern Marine Science and Engineering Guangdong Laboratory under Grant GML2019ZD0301, in part by the GDAS' Project of Science and Technology Development under Grant 2020GDASYL-20200103003, and in part by the National Data Sharing Infrastructure of Earth System Science.

ABSTRACT Sea surface temperature (SST) is a key factor for both climate and weather. Most studies focus on evaluation of satellite SSTs in different oceanic regions, but the performance of ERA5 reanalysis SST datasets (ERA5 SSTs) has not been systematically evaluated. In this article, buoy measurements from 46 National Data Buoy Center (NDBC) sites around the Pacific and the Atlantic are used to make an analysis of the deviations of the ERA5 SSTs on an hourly basis and its variations on a daily basis. Overall, ERA5 SSTs have a global coverage with a −0.04 °C bias and 4.60 °C standard deviation in the study area. It is worthwhile to notice that ERA5 SSTs exhibit significant differences in the amplitude and the phasing of their spatial patterns. The products are found to meet the accuracy criterion, except in near coastal areas, which may result from the near-coastal mixture effect and the warm SST. The results reveal that ERA5 SSTs completely capture the diurnal variability of SST under all wind speed conditions, especially in the situation when wind speed is above 6 m/s. There is a slight cold bias when wind speed is below 6m/s, indicating that ERA5 SSTs are not affected by solar radiation heating. These findings contribute to the sensible use of ERA5 SSTs around the Pacific and the Atlantic.

INDEX TERMS Accuracy evaluation, buoy measurements, ERA5, reanalysis product, sea surface temperature.

I. INTRODUCTION

Sea surface temperature (SST) is a key climate and weather factor which is important for the exchange of energy, momentum and moisture between the ocean and the atmosphere [1]. It has been proved that SST variations influence species in the marine environment and climate components. For example, the ENSO cycle has a profound effect on global-scale weather and primary productivity [2], [3]. SST also affects the development and evolution of tropical storms and hurricanes and is correlated with nutrient concentration [4], [5].

The associate editor coordinating the review of this manuscript and approving it for publication was Jiachen Yang.

Previous studies have demonstrated that SST has increased at global scale during recent decades [6], [7], while regional studies show that SST exhibits substantial spatiotemporal variations [8]–[11]. For example, increasing SST may display larger variations in shallow waters such as gulfs than in deep water areas [12]. Since SST is one of the critical determinants of air-sea interactions and climate variability, long-term monitoring of SST is necessary for understanding both the causes and results of climate change, as well as providing an important SST-dependent feedback mechanism via evaporation [13]. Currently, three kinds of SSTs (in situ observations, satellite, and reanalysis) are mainly used in practice. However, different SSTs perform fairly uniformly

globally or in basin-wide regions [14]. For example, mean SST differences in excess of 2 °C are consistently observed in the Arctic Ocean [15].

The buoy measurement and satellite-based SSTs suffer from several limitations. Buoy measurements lack the global coverage which can be compensated by satellite monitoring. The infrared remotely sensed SSTs have both spatial and temporal biases, affected by atmospheric aerosols, and incomplete removal of cloud contamination [16]. Microwave remotely sensed SSTs can overcome these drawbacks, but is limited by decreased sensitivity at high wind speeds and a relatively poor spatial resolution of 50 kilometers. Reanalysis data provides a long time series of SST by combining historical records with geophysical fluid-dynamical models based on data assimilation techniques [17]. Reanalysis SST data is widely applied for both climate change research and operational forecasting [3], [18]. However, most studies focus on evaluation of satellite-based SST products in different regions [19]–[21], while paying little attention to reanalysis data of SST.

The European Centre for Medium-Range Weather Forecasts (ECMWF) recently has released the fifth-generation reanalysis data product- European Centre for Medium Range Weather Forecasts Reanalysis 5 (ERA5), including SST. A recent study has analyzed the performance of solar radiations of the ERA5 reanalysis dataset [22]. The ERA5 reanalysis SST datasets (ERA5 SSTs) are mostly identical with external analysis data that are independent of the ERA5 data assimilation system, such as HadISST and OSTIA [23]. However, most existing studies on these datasets [23], [24] lack the evaluation of the SST data, and a quantitative evaluation of the ERA5 SSTs at site scale has not been carried out yet. In this study, the spatiotemporal uncertainties in hourly ERA5 SSTs around the Pacific and the Arctic are evaluated based on buoy retrievals from the National Data Buoy Center (NDBC). The deviations at different time scales and locations are quantitatively displayed. Such analyses and comparisons are relevant for understanding the causes of the errors, rational applications of the reanalysis products, and potential improvements of next-generation products.

II. DATA AND METHODS

A. DATA SOURCES AND PREPARATION

The ECMWF provides a global numerical description of the recent climate by combining models with observations. ERA5 is the latest reanalysis dataset at ECMWF, including SST. ERA5 has higher spatial resolution (30 km) than its predecessor ERA-Interim (79 km) [25] and has a revised data assimilation system and improved model physics [18]. ERA5 reanalysis SST data is an interpolated, gridded SST product, assimilating with a four-dimensional variational system [26]. ERA5 SSTs during the whole year of 2018 (from 01/01/2018 to 31/12/2018) as used in this study are available in NetCDF format, and can be downloaded from the ECMWF. The datasets are created with a valid time in the month, between 00 and 23 UTC. In this paper, in order to analyze the diurnal variations, UTC time is converted to the local time.

SSTs retrieved by NDBC buoys are used to evaluate the ERA5 SSTs. These data are collected and released by NOAA/NDBC (https://www.ndbc.noaa.gov/). The NDBC buoy measurements are collected hourly, using paired electronic thermistors, starting around 1975, showing time in UTC [27]. The precision of SST measurements made on NDBC buoys using electronic thermistors is ±0.08 °C for an individual hourly measurement, based on duplicate sensor comparisons [27], and the standard error for a monthly average is quite small [6]. Since the depth of the sensor varies with the buoy, the temperatures measured by buoy hulls gauge the average temperature of the water around the hull [27]. There are 46 buoy sites providing effective observations in 2018, and hourly observations for the whole year of 2018 are employed in this research. In Figure 1, the positions of NDBC buoy sites with effective observations in 2018 are displayed. The annual mean SST range is from approximately −1.79 °C to 24.6 °C. UTC time is also converted to the local time.

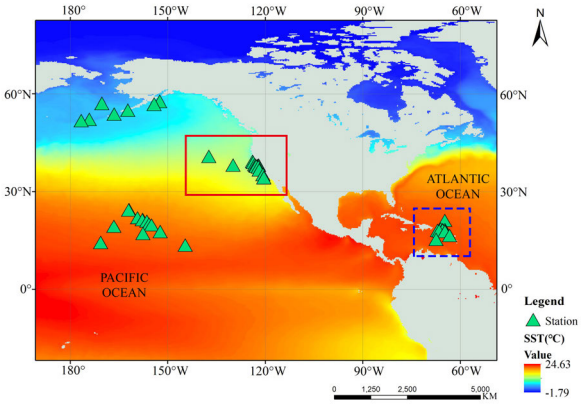

FIGURE 1. Continuous spatial distribution of the yearly SST and positions of the available buoy sites from ERA5 around the Pacific and the Atlantic in 2018.

Since NDBC buoys make point measurements throughout the day whereas the ERA5 SSTs are grid-averaged values, a matched set of the ERA5 SSTs and corresponding buoy measurements is constructed in this study. Collocation of the buoy measurements with the gridded ERA5 SSTs is straightforward. Buoy measurements are simply compared with the ERA5 SSTs at the grid cells containing the buoy position at that moment. In total, 313,266 pairs of collocated ERA5-buoy SSTs are obtained.

B. EVALUATION METRICS

In order to evaluate the ERA5 SSTs, several metrics are introduced to reveal whether the ERA5 SSTs overestimate or underestimate the real value, including the mean absolute error (MAE), mean bias error (MBE), root mean squared error (RMSE), standard deviation (STD) and coefficient of

determination (R^2). These statistic metrics are calculated by the following equations:

$$\mathrm{MAE} = \frac{1}{n}\sum_{i=0}^{n}\left|\widehat{SST}_i - SST_i\right| \tag{1}$$

$$\mathrm{MBE} = \frac{1}{n}\sum_{i=0}^{n}\widehat{SST}_i - SST_i \tag{2}$$

$$\mathrm{RMSE} = \sqrt{\frac{1}{n}\sum_{i=0}^{n}\left(\widehat{SST}_i - SST_i\right)^2} \tag{3}$$

$$STD = \sqrt{\frac{1}{n}\sum_{i=0}^{n}\left(\widehat{SST}_i - u\right)^2} \tag{4}$$

$$u = \frac{1}{n}\sum_{i=0}^{n}\widehat{SST}_i \tag{5}$$

$$R^2 = 1 - \sum_{i=0}^{n}\left(\widehat{SST}_i - SST_i\right)^2 \Bigg/ \sum_{i=0}^{n}\left(SST_i - \overline{SST}\right)^2 \tag{6}$$

where n is the total number of SST samples indexed by i, SST represents the observed value with the mean value $\overline{SST}$, and $\widehat{SST}$ is the predicted value from the ERA5 SST.

C. TAYLOR DIAGRAMS

Taylor diagram can provide a graphically means of summarizing the relative accuracies of several competing products [28], which is more succinct and clearer than analogous tabular presentation for conveying information [21]. In this study, Taylor diagrams are introduced to reflect the evaluation results in different aspects. In its basic form, a Taylor diagram is a two-dimensional scatter plot in which discrete points give an indication of how closely various ERA5 SSTs resemble the NDBC observations in terms of RMSE, STD and R^2 all at once. In addition, using color scheme can introduce a fourth dimension into the figure, with different color representing different value range of MAE.

The Taylor diagram is built by plotting a triangle in a rectangular coordinate system with one vertex at the origin, and the other two vertices representing the buoy measurements, and the corresponding ERA5 SST matchups, respectively. It is worthwhile mentioning that the Taylor diagram just provides information about the centered errors, instead of the overall bias [28].

III. RESULTS AND DISCUSSION

As ERA5 is the new generation product of ERA-interim, the accuracies of ERA-interim and ERA5 are evaluated and compared at first. Since ERA-interim does not provide hourly SST, the evaluation is performed on a daily scale, using daily NDBC buoy measurements as ground truth data. As shown in Figure 2, the green line represents ERA-interim SST, the red line represents ERA5 SST, the blue line represents NDBC buoy SST, and the accuracy is labeled in the upper left corner. Overall, the ERA5 SSTs correlated with ground truth data better than ERA-interim, with smaller MAE (0.44 versus 1.34), smaller RMSE (0.66 versus 1.90) and higher correlation (0.86 versus 0.80). Especially, ERA-interim SSTs exhibit

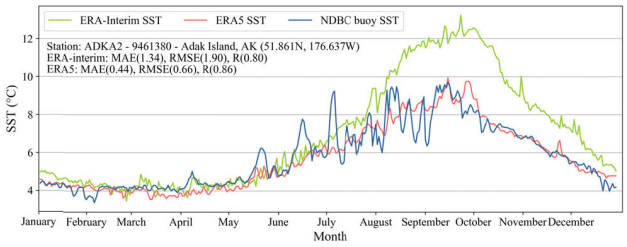

FIGURE 2. The daily SSTs of ERA-interim, ERA5 versus NDBC observations of ADKA2 station in 2018.

a significant overestimation from August to December. This is because that ERA5 reanalysis data uses a more recent model and data assimilation system, which can obtain more accurate STTs [29].

Figure 3a shows the density plot of the hourly coincident NDBC buoy and ERA5 SSTs. Overall, ERA5 hourly SSTs is well correlated to the NDBC buoy measurements with R^2 of 0.80. ERA5 SSTs appear to have a cold bias relative to the buoy, with a mean bias of −0.04 °C. This deviation might correspond to different regimes, such as coastal water, northerly waters, and extreme weather [21]. Martin *et al.* [30] have shown that differences among satellite-based SST products tended to be accentuated near coastal and strong gradient regions, and the uncertainties on coastal buoys exceed the global scale by about 0.3 K. In this case, the accuracies at each buoy are calculated in this study, as shown in Figure 4, where obvious geographical differences are observed. The ERA5 SSTs correlate fairly poorly with buoy measurements at near-costal buoys. However, the matchups in the region shown in Figure 1 with a blue dotted box, which is also near costal, demonstrate low MAEs and RMSEs. Therefore, in order to analyze whether the performance of ERA5 SSTs has longitudinal or latitudinal zonality, the matchups are grouped by the latitude and longitude of buoy, respectively. The results (Figure 5a and 5b) demonstrate that the correlation (R^2) between ERA5 and buoy SSTs exhibits no significant trend while the MAEs and RMSEs show an obvious increase between 25°N and 40°N, as well as between 60°W and 120°W, containing matchups shown in Figure 1 with a

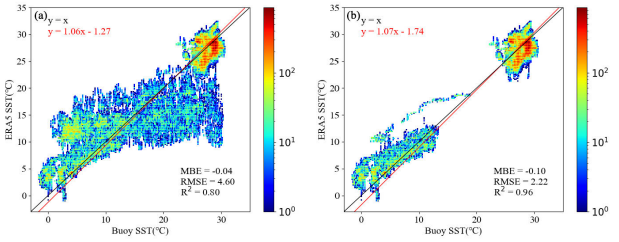

FIGURE 3. Density plot of the hourly ERA5 SSTs versus NDBC observations in 2018. Black solid line is the 1:1 line. Red solid line is the fitted regression line, and the expression is labeled in the upper left corner. (a) the accuracy including all matchups. (b) the accuracy excluding measurements displayed with a red box in Figure 1.

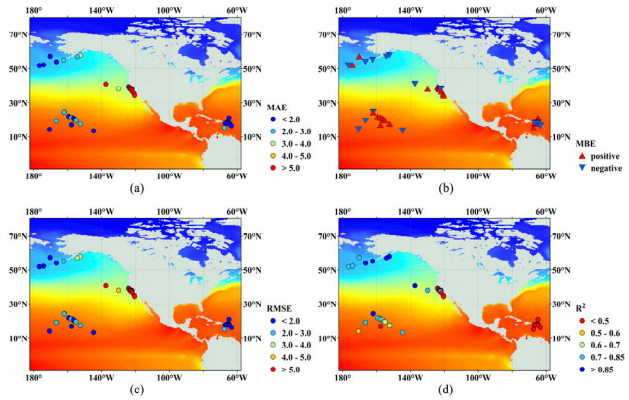

FIGURE 4. Spatial variation of the accuracy of the hourly ERA5 SSTs relative to NDBC buoy SSTs. (a) MAE. (b) MBE (showing whether MAE is positive or negative). (c) RMSE. (d) R^2.

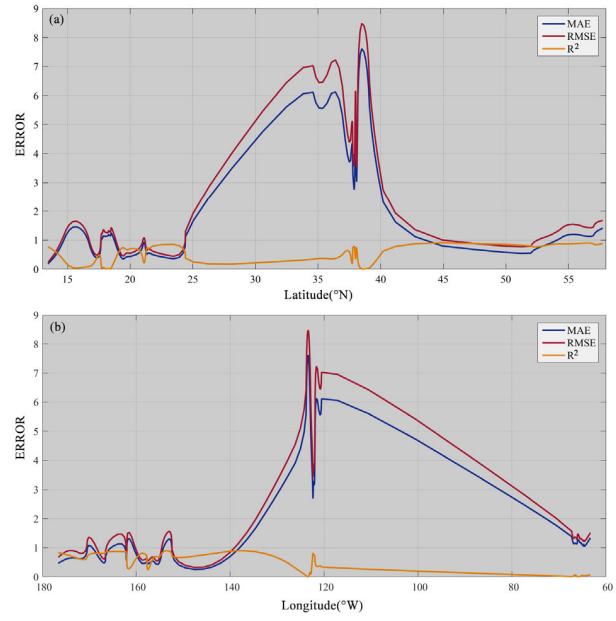

FIGURE 5. The accuracies of ERA5 SST change with latitude and longitude. The intersection area with large error contains buoys shown in Figure 1 with a red box.

red solid box. This indicates that the bad performance of ERA5 SSTs in the region shown in Figure 1 with a red box is not only due to the near-coastal mixture effect, but also is potentially related to warm SST, as a high-latitude negative bias has also been found in previous studies [21], [31]. If these match-up observations (those in the red box of Figure 1) are excluded from the study, the performance of ERA5 SSTs would be obviously improved (Figure 3b).

Daily variations of SST compared with ERA5 SSTs are calculated under two situations: (1) daily SSTs averaged over all the 46 buoys (Figure 6a), (2) daily SSTs averaged without 16 buoys located in the region shown in Figure 1 with a red box (Figure 6b). Figure 6a shows that ERA5 product underestimates daily SST in cold season and overestimates SST

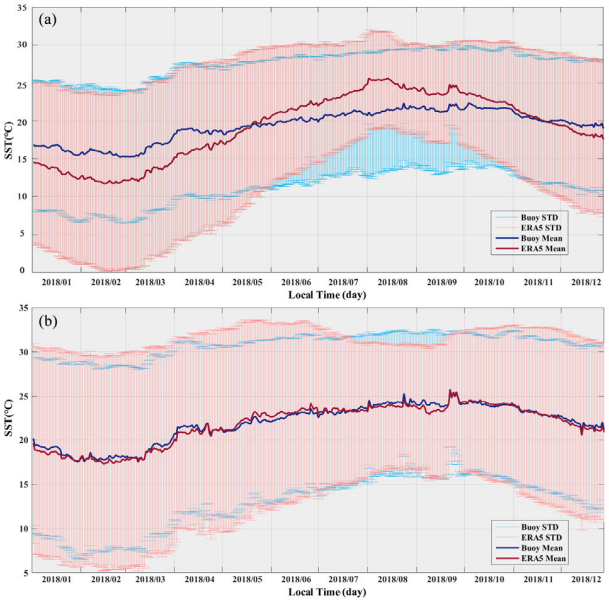

FIGURE 6. Time-series variations of ERA5 and NDBC buoy SSTs in 2018. Error bar show standard deviation for each daily mean SST. (a) Daily variation averaged over all the 46 buoys. (b) Daily variation averaged without 16 buoys.

in warm season. In contrast, this warm/cold bias disappears in Figure 6b. This implies that considering buoys in the red box of Figure 1 may lead to a total misunderstanding of the overall quality of the ERA5 SST product. In order to make more objective evaluation of ERA5 SSTs in other regions, the matchup data pairs mentioned above are excluded in the following analysis.

To evaluate the temporal variation more clearly, the accuracies of monthly and seasonal ERA5 SSTs are displayed with a Taylor diagram (Figure 7). The merits of different months or seasons can be inferred visually just by inspecting their position in the Taylor diagram. The closer the label representing the month/season is to the x-axis and y-axis, the better the agreement between the two datasets (ERA5 SSTs lying near the x-axis and y-axis have relatively high correlation and low STD). The closer the label to the center of the green line circle, the lower the RMSE value is. MAE is also displayed with the color of the label (from deep blue to bright yellow). The brighter the color is, the worse the performance is. As can be seen in Figure 7, ERA5 SSTs correlate very well with buoy measurements on both monthly and yearly scale. On the monthly scale, R^2 values are larger than 0.9 over the whole 12 months. The ERA5 SSTs in October has the smallest MAE and RMSE, while January suffers the largest MAE and RMSE, and December has the smallest standard deviation. On the yearly scale, all R^2 values are above 0.95, ERA5 SSTs perform best in autumn while worst in spring, and the SST has the smallest dispersion in winter.

Estimation of diurnal change in SST is of great importance for climate and air-sea interaction studies because it affects the air-sea heat fluxes directly [20]. Clayson and

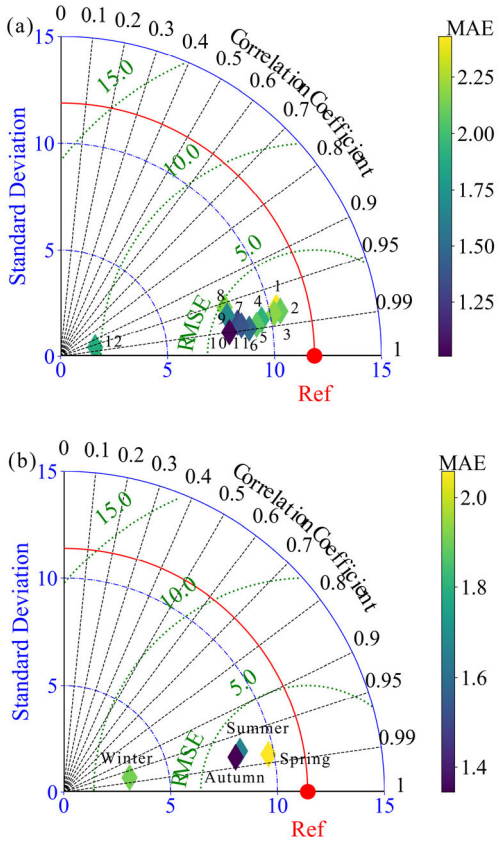

FIGURE 7. Taylor diagrams showing differences between grouped SST considering matchups of different months (a) and seasons (b) in 2018.

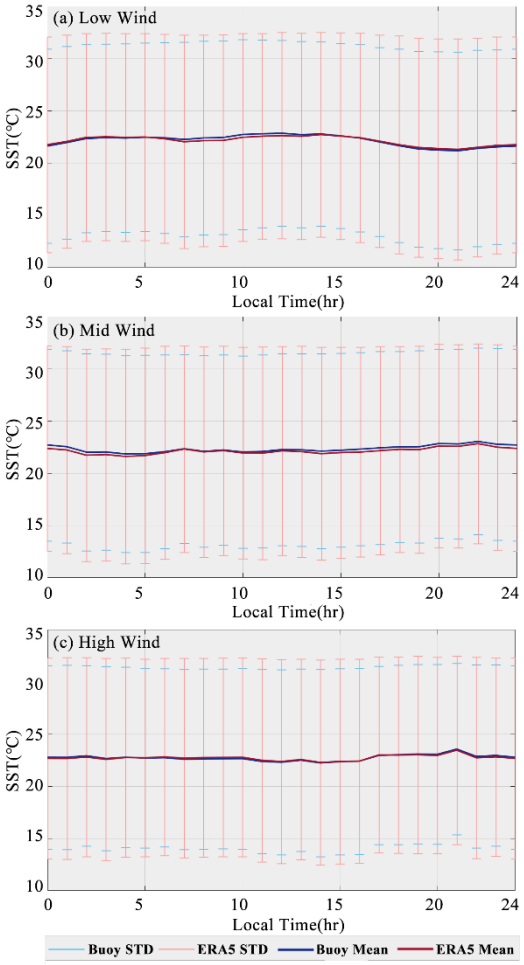

FIGURE 8. The ERA5 and NDBC buoy diurnal cycles: mean difference and standard deviation. (a) wind speed below 3m/s. (b) wind speed between 3m/s and 6m/s. (c) wind speed above 6m/s.

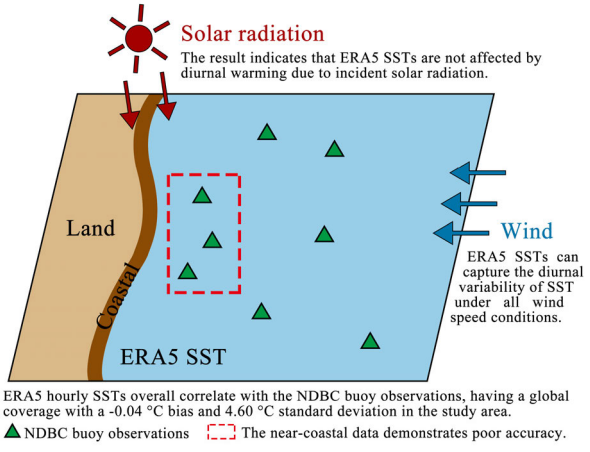

FIGURE 9. Summary of main findings.

Bogdanoff [32] find that the effect of diurnal change in SST on global climatological heat fluxes is 4.45 W/M^2 on average. So, the capability of capturing diurnal change of ERA5 SSTs is analyzed in this study. Additionally, several studies have suggested that the diurnal effect can be minimized by excluding daytime SSTs at wind speeds which is less than 6 m/s [13], [33]. We examine the diurnal variability of ERA5 and the buoy SSTs to directly verify this suggestion.

Figures 8a-8c show the results for three cases: (1) only matchup data with wind speeds below 3 m/s, when thermal stratification in the upper ocean layers will complicate the skin-bulk difference, (2) only matchup data with wind speeds between 6 and 10 m/s, when enhanced vertical mixing in the upper ocean due to wind-introduced mixing should stabilize the skin to sub-skin relationship, and (3) only matchup data with wind speeds above 10 m/s, when sub-skin temperature will decrease due to high wind-introduced upwelling and skin SST mixes with sub-skin SST thoroughly. Overall, ERA5 SSTs can capture the diurnal variation very well under different wind speed conditions, with biases ranging from −0.14 °C (at wind speeds below 3 m/s) to 0.34 °C (at wind speeds between 3 m/s and 6 m/s), although the standard deviation is slightly larger than buoy measurements (ranging from −1.16 °C to −0.64 °C). ERA5 SSTs coincide best with buoys in the case when wind speed exceeds 6 m/s. A negative bias occurs in daytime observations (between 6 A.M. and 1 P.M.) and is related to low wind speeds (below 3 m/s), and the same situation happens between 1 P.M. and 5 A.M.

at moderate wind speeds. This indicates that ERA5 SSTs are not affected by diurnal warming due to incident solar radiation, and may be related to the fact that the depth representations of ERA5 and buoy SSTs are different.

IV. CONCLUSION

In this study, the ERA5 SST product, newly released by ECMWF, is evaluated from different aspects, including temporal, spatial and potential causes. The NDBC buoys provide a unique, and valuable, verification dataset, giving great confidence in the results. Overall, ERA5 SSTs are of comparable accuracy, with a -0.04 °C bias and 4.60 °C standard deviation around the Pacific and the Arctic, when compared to NDBC buoys. It is worthwhile to notice that ERA5 SSTs exhibit significant differences in the amplitude and the phasing of their spatial patterns. Products are found to meet the accuracy criterion except in near coastal regions. Especially in the region marked in Figure 1 with a red box, ERA5 SSTs exhibit rather poor performance. The same situation occurs in daily SST variation, considering buoys mentioned above may lead to serious misunderstandings about the overall accuracy of ERA5 SST product.

One single statistical metric cannot fully reflect the performance of ERA5 SSTs in all respects, thus a variety of metrics are chosen to make the evaluation and different diagrams are employed to explicitly represent the evaluation results. Taylor diagrams can provide an intuitively graphical summary of four different statistics (MAE, RMSE, STD and R^2) which demonstrates different strengths and weaknesses in the ERA5 SSTs. The results have suggested that ERA5 SSTs are in agreement with buoy measurements both on monthly or seasonal scale around the Pacific and the Atlantic. The main findings of this study are shown in Figure 9.

It has been reported that satellite-based SST data is significantly affected by the wind speed. However, the results demonstrate that ERA5 SSTs can capture the diurnal variability of SST very well under all wind speed conditions, no exception in the situation when wind speed is above 6 m/s. Actually, there is a slight cold bias while wind speed is below 6m/s, indicating that ERA5 SSTs are not affected by diurnal warming due to incident solar radiation.

The ERA5 SSTs achieve an overall agreement with the NDBC buoy measurements, while its accuracy varies under different temporal, spatial and meteorological conditions. The main findings of this article provide a foundation for researches based on ERA5 SSTs around the Pacific and the Atlantic.

REFERENCES

[1] F. J. Wentz, C. Gentemann, D. Smith, and D. Chelton, "Satellite measurements of sea surface temperature through clouds," *Science*, vol. 288, no. 5467, pp. 847–850, 2000.
[2] Brander, K, "Global fish production and climate change," *Proc. Nat. Acad. Sci. USA*, 2007, vol. 104, no. 50, pp. 19709–19714.
[3] R. Noori, F. Tian, R. Berndtsson, M. R. Abbasi, M. V. Naseh, A. Modabberi, A. Soltani, and B. Kløve, "Recent and future trends in sea surface temperature across the persian gulf and gulf of oman," *PLoS ONE*, vol. 14, no. 2, Feb. 2019, Art. no. e0212790.
[4] M. A. Cane, A. C. Clement, A. Kaplan, Y. Kushnir, D. Pozdnyakov, R. Seager, S. E. Zebiak, and R. Murtugudde, "Twentieth-century sea surface temperature trends," *Science*, vol. 275, no. 5302, pp. 957–960, Feb. 1997.
[5] K. A. Emanuel, "Thermodynamic control of hurricane intensity," *Nature*, vol. 401, no. 6754, pp. 665–669, Oct. 1999.
[6] R. K. Shearman and S. J. Lentz, "Long-term sea surface temperature variability along the U.S. east coast," *J. Phys. Oceanogr.*, vol. 40, no. 5, pp. 1004–1017, May 2010.
[7] C. Sheppard, M. Al-Husiani, F. Al-Jamali, F. Al-Yamani, R. Baldwin, J. Bishop F. Benzoni, E. Dutrieux, N. K. Dulvy, S. R. V. Durvasula, and D. A. Jones, "The gulf: A young sea in decline," *Mar. Pollut. Bull.*, vol. 60, no. 1, pp. 13–38, 2010.
[8] B. Riegl, "Effects of the 1996 and 1998 positive sea-surface temperature anomalies on corals, coral diseases and fish in the arabian gulf (Dubai, UAE)," *Mar. Biol.*, vol. 140, no. 1, pp. 29–40, Jan. 2002.
[9] M. Falvey and R. D. Garreaud, "Regional cooling in a warming world: Recent temperature trends in the southeast pacific and along the west coast of subtropical South America (1979–2006)," *J. Geophys. Res.*, vol. 114, no. D4, pp. 217–221, 2009.
[10] S. E. Lluch-Cota, M. Tripp-Valdez, D. B. Lluch-Cota, J. J. Bautista-Romero, D. Lluch-Belda, J. Verbesselt, and H. Herrera-Cervantes, "Recent trends in sea surface temperature off mexico," *Atmósfera*, vol. 26, no. 4, pp. 537–546, Oct. 2013.
[11] A. Shirvani, "Change point detection of the persian gulf sea surface temperature," *Theor. Appl. Climatol.*, 2015, vol. 202, no. 2, pp. 1–5, 2015.
[12] I. M. Belkin, "Rapid warming of large marine ecosystems," *Prog. Oceanogr.*, vol. 81, nos. 1–4, pp. 207–213, Apr. 2009.
[13] C. L. F. J. G. Wentz, C. A. Mears, and D. K. Smith, "*In situ* validation of tropical rainfall measuring mission microwave sea surface temperatures," *J. Geophys. Res.*, vol. 109, no. C4, 2004, Art. no. C04021.
[14] S. L. Castro, G. A. Wick, and W. J. Emery, "Evaluation of the relative performance of sea surface temperature measurements from different types of drifting and moored buoys using satellite-derived reference products," *J. Geophys. Res., Oceans*, vol. 117, no. C2, Feb. 2012, Art. no. C02029.
[15] P. Dash, A. Ignatov, M. Martin, C. Donlon, B. Brasnett, R. W. Reynolds, V. Banzon, H. Beggs, J. F. Cayula, Y. Chao, and R. Grumbine, "Group for high resolution sea surface temperature (GHRSST) analysis fields inter-comparisons—Part 2: Near real time Web-based level 4 SST quality monitor (L4-SQUAM)," *Deep Sea Res. II, Topical Stud. Oceanogr.*, vols. 77–80, pp. 31–43, Nov. 2012.
[16] W. J. Emery, Y. Yu, G. A. Wick, P. Schluessel, and R. W. Reynolds, "Correcting infrared satellite estimates of sea surface temperature for atmospheric water vapor attenuation," *J. Geophys. Res.*, vol. 99, no. C3, p. 5219, 1994.
[17] J. W. Hurrell and K. E. Trenberth, "Global sea surface temperature analyses: Multiple problemsand their implications for climate analysis, modeling, and reanalysis," *Bull. Amer. Meteorolog. Soc.*, vol. 80, no. 12, pp. 2661–2678, Dec. 1999.
[18] S. A. Josey, M. F. Jong, M. Oltmanns, G. K. Moore, and R. A. Weller, "Extreme variability in irminger sea winter heat loss revealed by ocean observatories initiative mooring and the ERA5 reanalysis," *Geophys. Res. Lett.*, vol. 46, no. 1, pp. 293–302, Jan. 2019.
[19] T. Hihara, M. Kubota, and A. Okuro, "Evaluation of sea surface temperature and wind speed observed by GCOM-W1/AMSR2 using *in situ* data and global products," *Remote Sens. Environ.*, vol. 164, pp. 170–178, Jul. 2015.
[20] H. Tomita, Y. Kawai, M. F. Cronin, T. Hihara, and M. Kubota, "Validation of AMSR2 sea surface wind and temperature over the kuroshio extension region," *Sola*, vol. 11, pp. 43–47, Apr. 2015.
[21] S. L. Castro, G. A. Wick, and M. Steele, "Validation of satellite sea surface temperature analyses in the beaufort sea using UpTempO buoys," *Remote Sens. Environ.*, vol. 187, pp. 458–475, Dec. 2016.
[22] H. Jiang, Y. Yang, Y. Bai, and H. Wang, "Evaluation of the total, direct, and diffuse solar radiations from the ERA5 reanalysis data in China," *IEEE Geosci. Remote Sens. Lett.*, vol. 17, no. 1, pp. 47–51, Jan. 2020.
[23] H. Hersbach, B. Bell, P. Berrisford, S. Hirahara, A. Horányi, J. Muñoz-Sabater, J. Nicolas, C. Peubey, R. Radu, D. Schepers, and A. Simmons, "The ERA5 global reanalysis," *Quart. J. Royal Meteorolog. Soc.*, vol. 146, no. 730, pp. 1999–2049, 2020.

[24] S. Hirahara, M. A. Balmaseda, E. D. Boisseson, and H. Hersbach, "26 sea surface temperature and sea ice concentration for ERA5," Eur. Centre Medium Range Weather Forecasts, Berkshire, U.K., ERA Rep. Ser. 26, 2016.
[25] D. P. Dee, S. M. Uppala, A. J. Simmons, P. Berrisford, P. Poli, S. Kobayashi, U. Andrae, M. A. Balmaseda, G. Balsamo, D. P. Bauer, and P. Bechtold, "The ERA?Interim reanalysis: Configuration and performance of the data assimilation system," *Quart. J. Roy. Meteorolog. Soc.*, vol. 2011, vol. 137, no. 656, pp. 553–597.
[26] F. Rabier, J.-N. Thépaut, and P. Courtier, "Extended assimilation and forecast experiments with a four-dimensional variational assimilation system," *Quart. J. Roy. Meteorolog. Soc.*, vol. 124, no. 550, pp. 1861–1887, Jul. 1998.
[27] *Handbook of Automated Data Quality Control Checks and Procedures of the National Data Buoy Center*, NDBC Tech, Shanghai, China, 2003.
[28] K. E. Taylor, "Summarizing multiple aspects of model performance in a single diagram," *J. Geophys. Res., Atmos.*, vol. 106, no. D7, pp. 7183–7192, Apr. 2001.
[29] C. Albergel, E. Dutra, S. Munier, J.-C. Calvet, J. Munoz-Sabater, P. de Rosnay, and G. Balsamo, "ERA-5 and ERA-interim driven ISBA land surface model simulations: Which one performs better?" *Hydrol. Earth Syst. Sci.*, vol. 22, no. 6, pp. 3515–3532, Jun. 2018.
[30] M. Martin, P. Dash, A. Ignatov, V. Banzon, H. Beggs, B. Brasnett, J. F. Cayula, J. Cummings, C. Donlon, C. Gentemann, and R. Grumbine, "Group for high resolution sea surface temperature (GHRSST) analysis fields inter-comparisons. Part 1: A GHRSST multi-product ensemble (GMPE)," *Deep-Sea Res., II, Topical Stud. Oceanogr.*, vol. 77, pp. 21–30, Nov. 2012.
[31] S. Dong, S. T. Gille, J. Sprintall, and C. Gentemann, "Validation of the advanced microwave scanning radiometer for the Earth observing system (AMSR-E) sea surface temperature in the southern ocean," *J. Geophys. Res.*, vol. 111, no. C4, pp. 1–16, 2006.
[32] C. A. Clayson and A. S. Bogdanoff, "The effect of diurnal sea surface temperature warming on climatological air–sea fluxes," *J. Climate*, vol. 26, no. 8, pp. 2546–2556, Apr. 2013.
[33] C. J. Donlon, P. J. Minnett, C. Gentemann, T. J. Nightingale, I. J. Barton, B. Ward, and M. J. Murray, "Toward improved validation of satellite sea surface skin temperature measurements for climate research," *J. Climate*, vol. 15, no. 4, pp. 353–369, Feb. 2002.

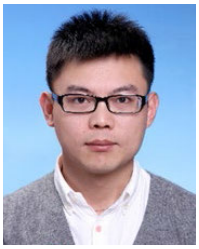

LING YAO received the Ph.D. degree from the State Key Laboratory of Resources and Environmental Information System, Institute of Geographic Sciences and Natural Resources Research (IGSNRR), Chinese Academy of Sciences (CAS), Beijing, China, in 2012. From September 2012 to December 2014, he was a Postdoctoral Fellow with CAS. He is currently an Associate Professor with IGSNRR, CAS. His research interests include remote sensing and spatio-temporal data mining.

JIAYING LU received the B.S. degree in geographic information systems from the Honors College, Nanjing Normal University, Nanjing, China, in 2019. She is currently pursuing the master's degree with the State Key Laboratory of Resources and Environmental Information System, Institute of Geographic Sciences and Natural Resources Research (IGSNRR), Chinese Academy of Sciences (CAS), Beijing, China. Her research interests include remote sensing and spatio-temporal data mining.

XIAOLIN XIA received the B.S. and M.S. degrees in geomatics from the University of Gävle, Sweden, in 2011 and 2013, respectively, and the Ph.D. degree in cartography and geographic information engineering from the Shandong University of Science and Technology, Qingdao, China, in 2017. From March 2014 to June 2017, she was a Visiting Doctoral Student with the State Key Laboratory of Resources and Environmental Information System, Institute of Geographic Sciences and Natural Resources Research (IGSNRR), Chinese Academy of Sciences (CAS), Beijing, China. She currently holds a postdoctoral position with the Guangzhou Institute of Geography, Guangzhou, China. Her research interests include environmental health, hydrologic remote sensing, and spatio-temporal data mining.

WENLONG JING received the Ph.D. degree from the State Key Laboratory of Resources and Environmental Information System, Institute of Geographic Sciences and Natural Resources Research (IGSNRR), Chinese Academy of Sciences (CAS), Beijing, China, in 2017. He is currently an Assistant Professor with the Guangzhou Institute of Geography. His research interests include hydrology remote sensing and machine learning techniques.

YANGXIAOYUE LIU received the B.S. degree in geography science from Shandong Normal University, Jinan, China, in 2013, the M.S. degree in cartography and geographical information system from the Shandong University of Science and Technology, Qingdao, China, in 2016, and the Ph.D. degree in cartography and geographical information system from the State Key Laboratory of Resources and Environmental Information System, Institute of Geographic Sciences and Natural Resources Research (IGSNRR), Chinese Academy of Sciences (CAS), Beijing, China, in 2019. She currently holds a postdoctoral position with the Guangzhou Institute of Geography, Guangzhou, China. Her research interests include satellite-based environment remote sensing and spatio-temporal data mining.